

Supplemental Information

Martini Coarse-Grained Force Field:

Extension to RNA

Jaakko J. Uusitalo, Helgi I. Ingólfsson, Siewert J. Marrink, and Ignacio Faustino

Supporting Information for:

Martini Coarse-Grained Force Field: Extension to RNA

J.J. Uusitalo^l, H.I. Ingólfsson^{l,†}, S.J. Marrink,^{l,}, I. Faustino^l.*

^lGroningen Biomolecular Sciences and Biotechnology Institute and Zernike Institute for Advanced Materials, University of Groningen, Nijenborgh 7, 9747 AG Groningen, The Netherlands.

[†]Current address: Lawrence Livermore National Laboratory, 7000 East Avenue, L-367, Livermore, CA 94550

**Correspondence: s.j.marrink@rug.nl*

Table S1. Sequences of the short ssRNAs used to parameterize the bonded interactions.

Sequence
AAAA
ACAC
AGAG
AUAU
CCCC
CUUG
GAAA
GAGA
GCAA
GCGA
GCGC
GGAA
GGGA
GGGG
GUAA
GUGA
GUUG
UACG
UCCG
UGCG
UGGU
UUCG
UUUU

Table S2. The Martini RNA bead mapping.

Bead name	Bead type	Mapped atoms
BB1	Q0	P, OP1/O1P, OP2/O2P, O5', O3'
BB2	SN0	C5', O4', C4
BB3	SNda	C3', C2', C1'
SC1 (adenine)	TN0	N9, C4
SC2 (adenine)	TA2	C2, N3
SC3 (adenine)	TA3	C6, N6, N1
SC4 (adenine)	TNa	C8, N7, C5
SC1 (cytosine)	TN0	N1, C6
SC2 (cytosine)	TY2	N3, C2, O2
SC3 (cytosine)	TY3	C5, C4, N4
SC1 (guanine)	TN0	N9, C4
SC2 (guanine)	TG2	C2, N2, N3
SC3 (guanine)	TG3	C6, O6, N1
SC4 (guanine)	TNa	C8, N7, C5
SC1 (uracil)	TN0	N1, C6
SC2 (uracil)	TT2	N3, C2, O2
SC3 (uracil)	TT3	C5, C4, O4

Table S3. The Martini RNA bonded parameters.

Beads	Type	Position of minimum ¹	Force constant ¹
BB1-BB2	1	0.363	20 000
BB2-BB3	1	0.202	40 000
BB3-BB1	1	0.354	10 000
BB1-BB2-BB3	2	117.0	175
BB2-BB3-BB1	2	95.0	105
BB3-BB1-BB2	2	93.0	75
BB1-BB2-BB3-BB1	2	0.0	3.5
BB2-BB3-BB1-BB2	1	0.0 ⁴	1
BB3-BB1-BB2-BB3	9	-10.0 ²	1.5
BB3-BB1-BB2-BB3	9	10.0 ²	1.5
BB3-ASC1	1	0.293	28 000
ASC1-ASC2	1	0.234	constraint
ASC2-ASC3	1	0.263	constraint
ASC2-ASC4	1	0.335	40 000
ASC3-ASC4	1	0.299	constraint
ASC4-ASC1	1	0.162	constraint
BB2-BB3-ASC1	2	101.0	260
BB3-ASC1-ASC2	2	153.0	90
BB3-ASC1-ASC4	2	135.0	185
ASC1-ASC2-ASC3	1	87.0	200
ASC1-BB3-BB1	2	160.0	15
ASC2-ASC1-ASC4	1	115.0	200
ASC2-ASC3-ASC4	1	74.0	200
ASC3-ASC4-ASC1	1	92.0	200
BB1-BB2-BB3-ASC1	2	180.0	1.5
BB2-BB3-ASC1-ASC2	1	-40.0 ²	4
BB2-BB3-ASC1-ASC2	2	180.0	2
BB2-BB3-ASC1-ASC4	1	-10.0 ²	5
BB2-BB3-ASC1-ASC4	2	80.0	0.5
ASC1-ASC2-ASC3-ASC4	2	0.0	10
BB3-CSC1	1	0.280	11 000
CSC1-CSC2	1	0.224	constraint
CSC2-CSC3	1	0.281	constraint
CSC3-CSC1	1	0.267	constraint

BB2-BB3-CSC1	2	94.0	230
BB3-CSC1-CSC2	2	103.0	170
BB2-CSC1-CSC3	1	155.0	100
CSC1-BB3-BB1	1	130.0	0.5
CSC1-CSC2-CSC3	1	61.0	200
CSC2-CSC1-CSC3	1	71.0	200
CSC2-CSC3-CSC1	1	47.0	200
BB1-BB2-BB3-CSC1	1	55.0 ²	3
BB1-BB2-BB3-CSC1	2	-130.0	1
BB2-BB3-CSC1-CSC2	2	180.0	3
BB2-BB3-CSC1-CSC2	1	0.0 ⁶	2
BB3-GSC1	1	0.292	20 000
GSC1-GSC2	1	0.296	constraint
GSC2-GSC3	1	0.291	constraint
GSC2-GSC4	1	0.385	40 000
GSC3-GSC4	1	0.296	constraint
GSC4-GSC1	1	0.162	constraint
BB2-BB3-GSC1	2	103.0	260
BB3-GSC1-GSC2	2	129.0	80
BB3-GSC1-GSC4	2	137.0	120
GSC1-GSC2-GSC3	1	72.0	200
GSC1-BB3-BB1	2	170.0	20
GSC2-GSC1-GSC4	1	117.0	200
GSC2-GSC3-GSC4	1	84.0	200
GSC3-GSC4-GSC1	1	96.5	200
BB1-BB2-BB3-GSC1	1	-20.0 ²	1
BB2-BB3-GSC1-GSC2	2	180.0	3.5
BB2-BB3-GSC1-GSC4	1	0.0 ²	5
GSC1-GSC2-GSC3-GSC4	2	0.0	10
BB3-USC1	1	0.286	18 000
USC1-USC2	1	0.224	constraint
USC2-USC3	1	0.289	constraint
USC3-USC1	1	0.276	constraint
BB2-BB3-USC1	2	95.0	225
BB3-USC1-USC2	2	99.0	200
BB2-USC1-USC3	1	155.0	100
USC1-BB3-BB1	1	180.0	5

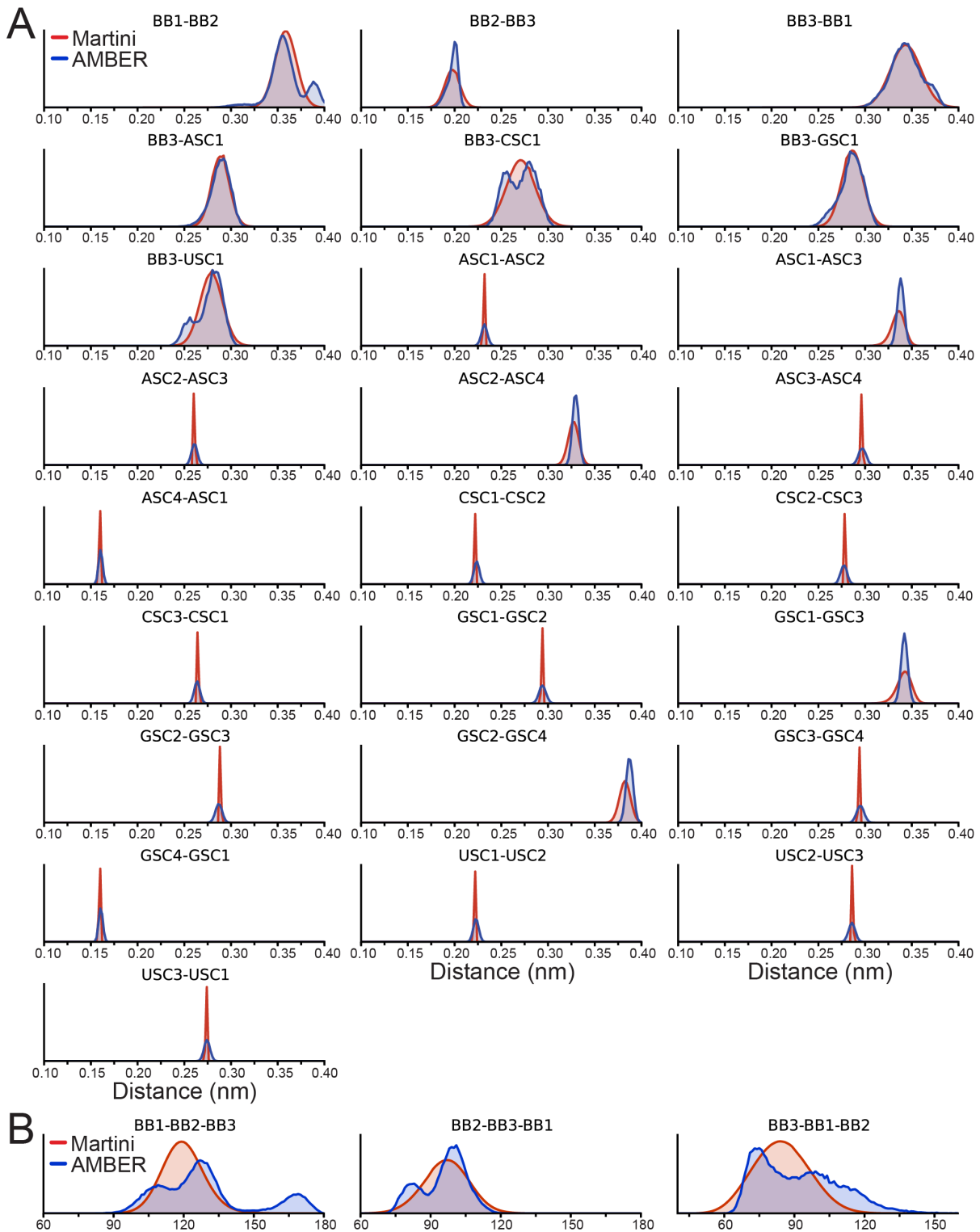
USC1-USC2-USC3	1	55.0	100
USC2-USC1-USC3	1	83.0	100
USC2-USC3-USC1	1	42.0	100
BB1-BB2-BB3-USC1	1	0.0 ²	2
BB2-BB3-USC1-USC2	2	180.0	4
BB2-BB3-USC1-USC3	1	0.0 ⁶	2

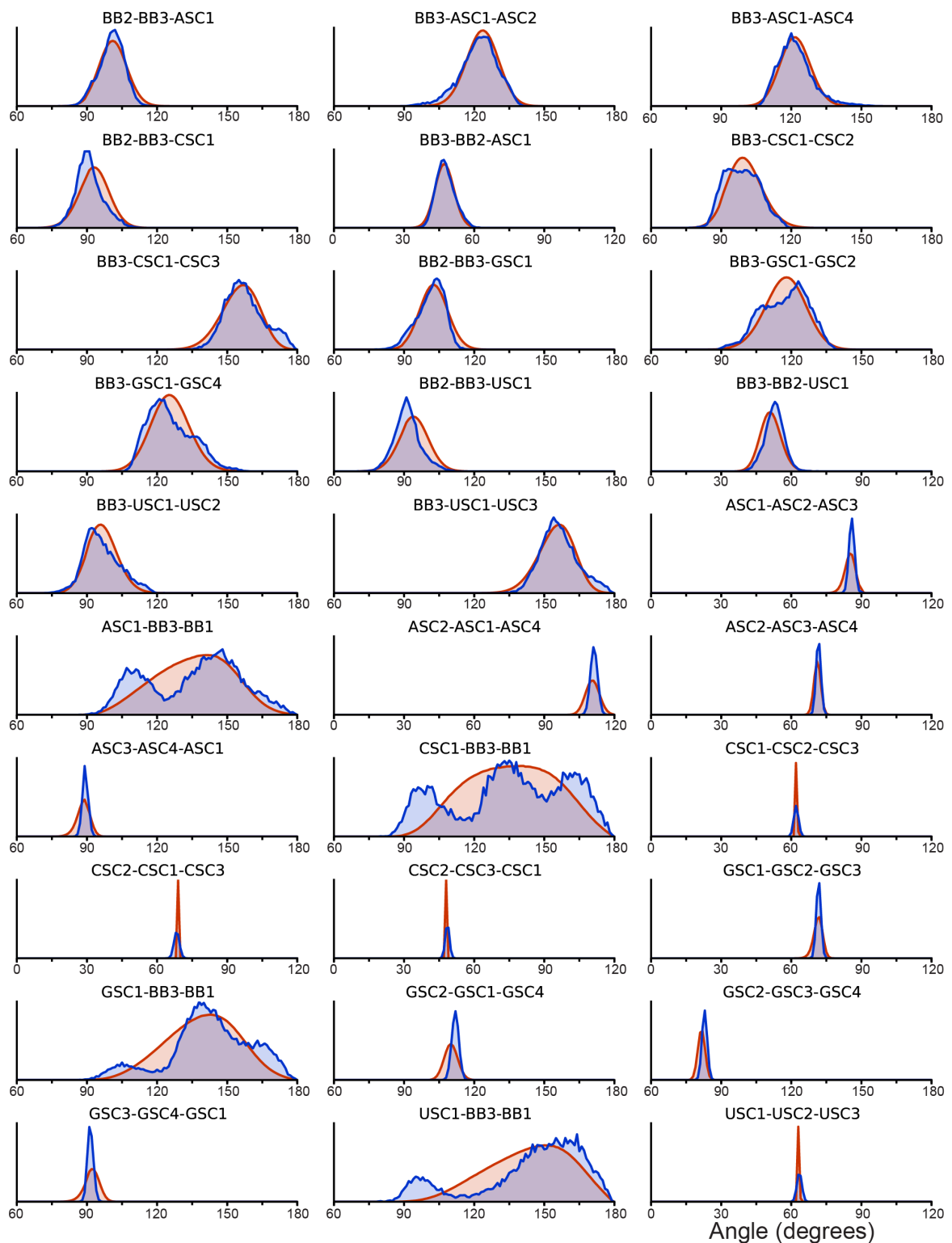
¹Units for the position of the minimum are nm (bonds) or degrees (angles), units for the force constants are $\text{kJ mol}^{-1} \text{nm}^{-2}$ (bonds), kJ mol^{-1} (angles), or $\text{kJ mol}^{-1} \text{rad}^{-2}$ (dihedrals). In addition to the standard exclusions of bonded neighbors, the second neighbors are also excluded in the backbone and the base beads are excluded from the backbone beads of the same residue.

²Multiplicity of the dihedral is 2. ³Multiplicity of the dihedral is 3. ⁴Multiplicity of the dihedral is 4. ⁶Multiplicity of the dihedral is 6.

Table S4. Sequence of the 100 base pair random dsRNA used for persistence length calculation. For comparison, the same sequence was used for the dsDNA molecule by changing the uracils by thymines.

Sequence
GGGUAAUCAGCCGUCUCCACCAACACACAACGCUAUCGGGUCAUAUUUAAGAUUCCGCAAUGGG ACUACUUAUAGGUUGCCUUAACGAUAUCCGCAACUUAAGUUGC GGAAUCGUUAAGGCAACCU AUAAGUAGUCCCCAUUGC GGAAUCUUUAUAUGACCCGAUAGCGUUGUGUUGGUUGGAGACGGC UGAUUACCCU





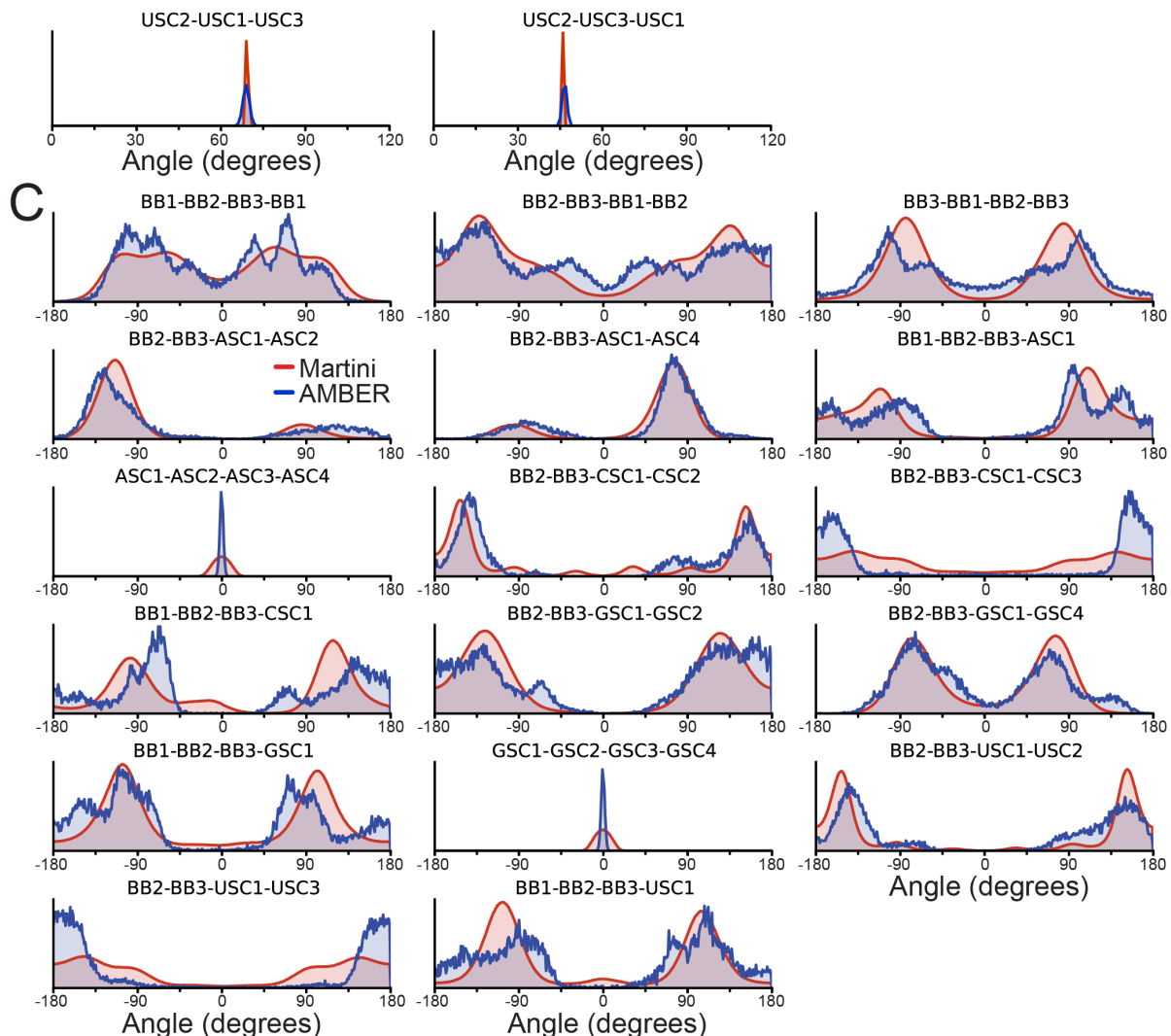


Figure S1. CG and AA distributions of bonded terms. The average distribution from Martini CG simulations is shown in red whereas the average AMBER AA distribution is in blue. The title of each subplot lists the beads that participate in the (A) bond, (B) angle or (C) dihedral distribution and the letter in the beginning of side chain beads denotes to which nucleobase the bead belongs to. Beads are named according to the naming scheme of Table S2.

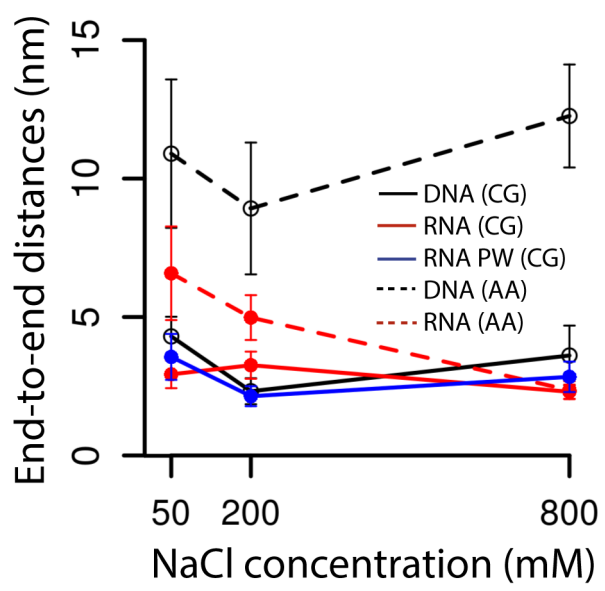


Figure S2. Comparison of end-to-end distances of single strand 40-mer polyT and polyU molecules. Values from CG simulations are shown as solid lines and from atomistic simulations as dashed lines.

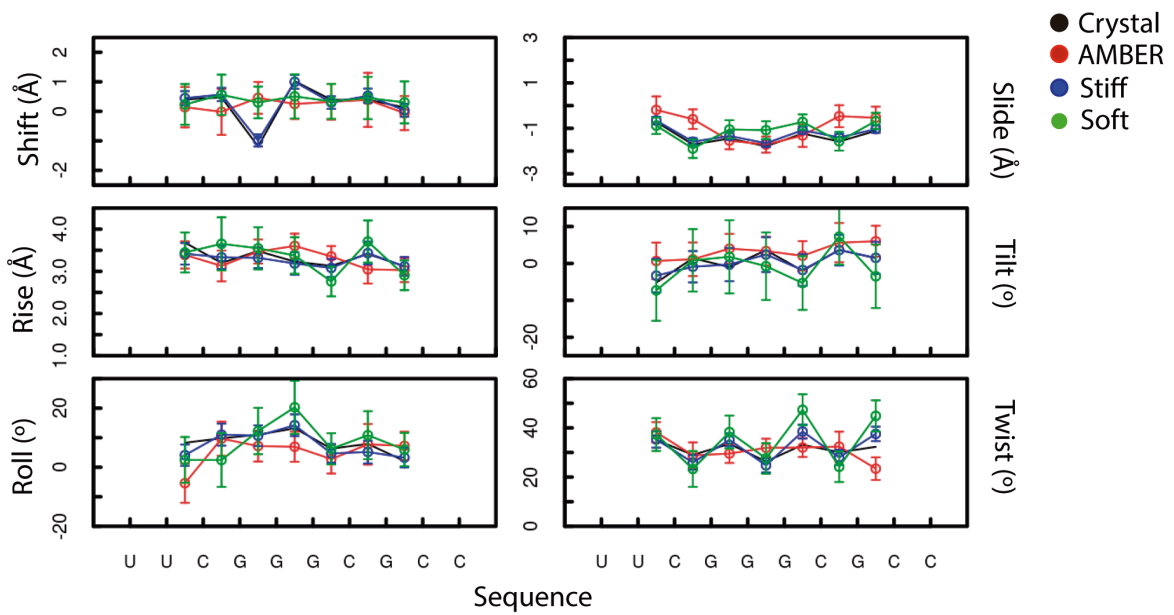


Figure S3. Base pair step helical parameters. Values obtained from 100 ns simulation of a 1FIX DNA:RNA hybrid molecule in 150 mM NaCl. The values from the crystal structure are in black, atomistic AMBER simulations in red, stiff RNA Martini model in blue and soft RNA Martini model in green.

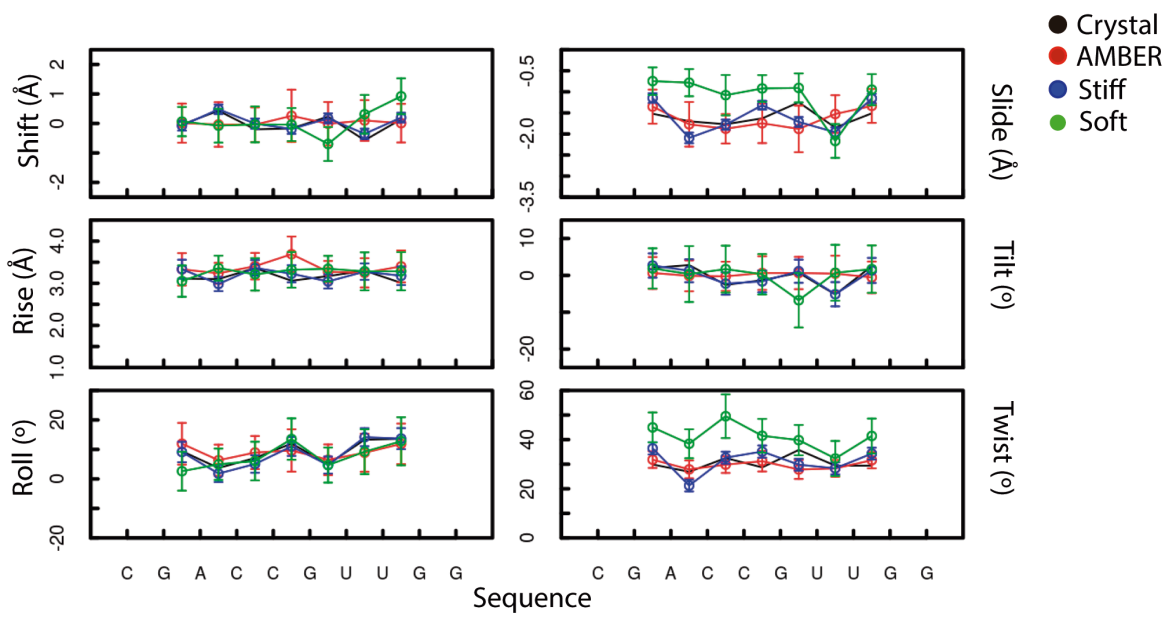


Figure S4. Base pair step helical parameters. Values obtained from 100 ns simulation of a 1QC0 dsRNA molecule in 150 mM NaCl. The values from the crystal structure are in black, atomistic AMBER simulations in red, stiff RNA Martini model in blue and soft RNA Martini model in green.

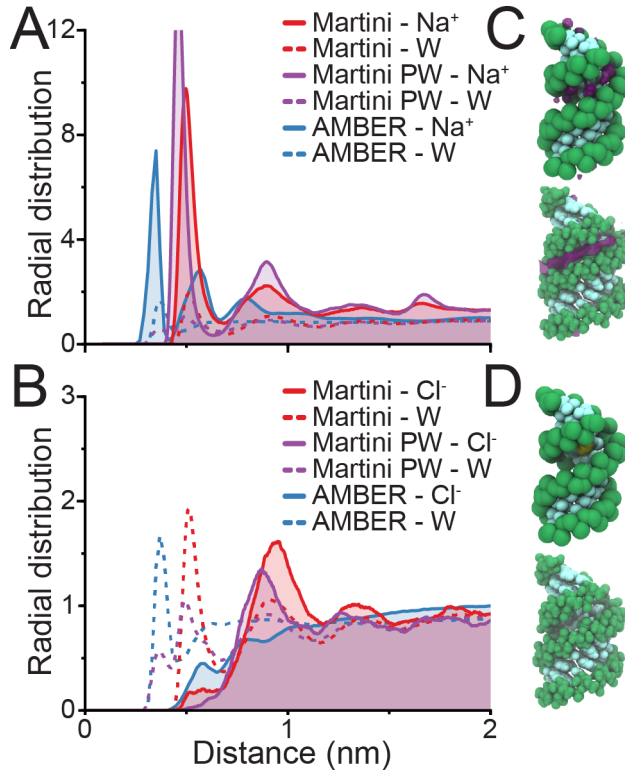


Figure S5. Ion distribution around dsRNA. The ion distribution around the phosphate beads of RNA for (A) sodium and (B) chloride from simulations in 1000 mM NaCl solution. Volume maps of locations most commonly occupied by sodium (C) and chloride (D) are shown for Martini (top) and AMBER (bottom) simulations.

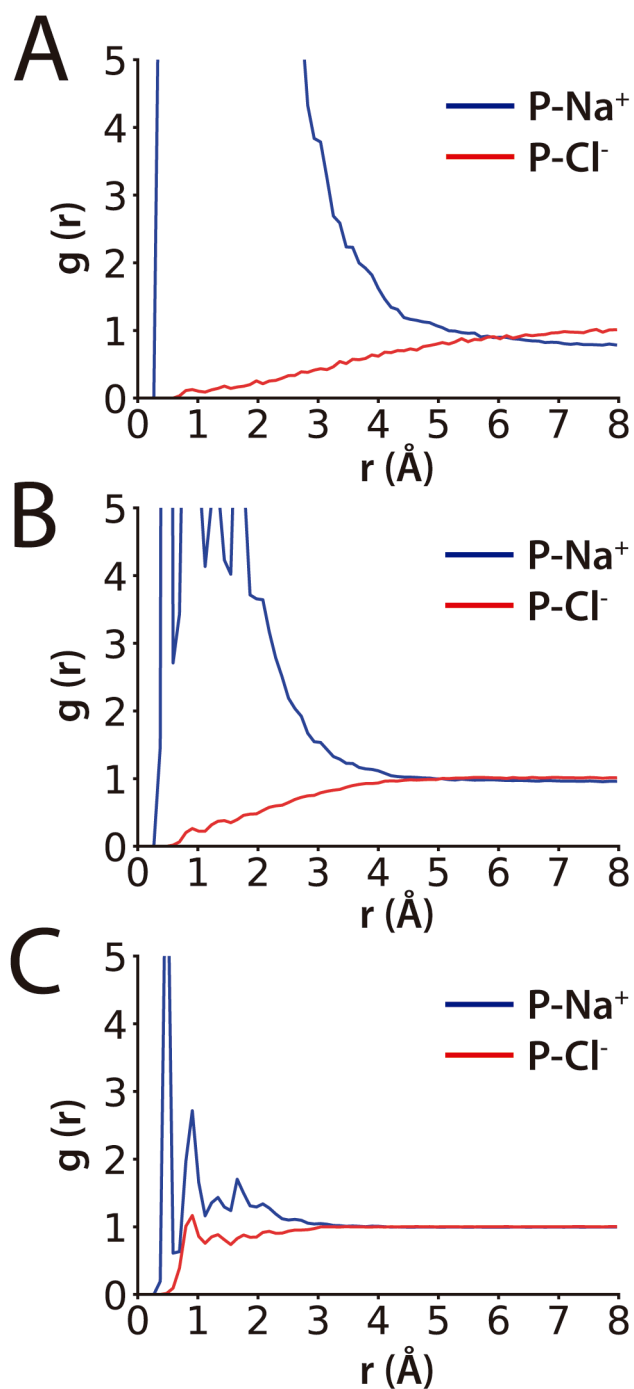


Figure S6. RNA phosphate-ions radial distribution functions for the 1RNA dsRNA molecule in a 190 Å box of 10 (A), 100 (B) and 1000 (C) mM NaCl. Simulations were run with the polarizable water model.

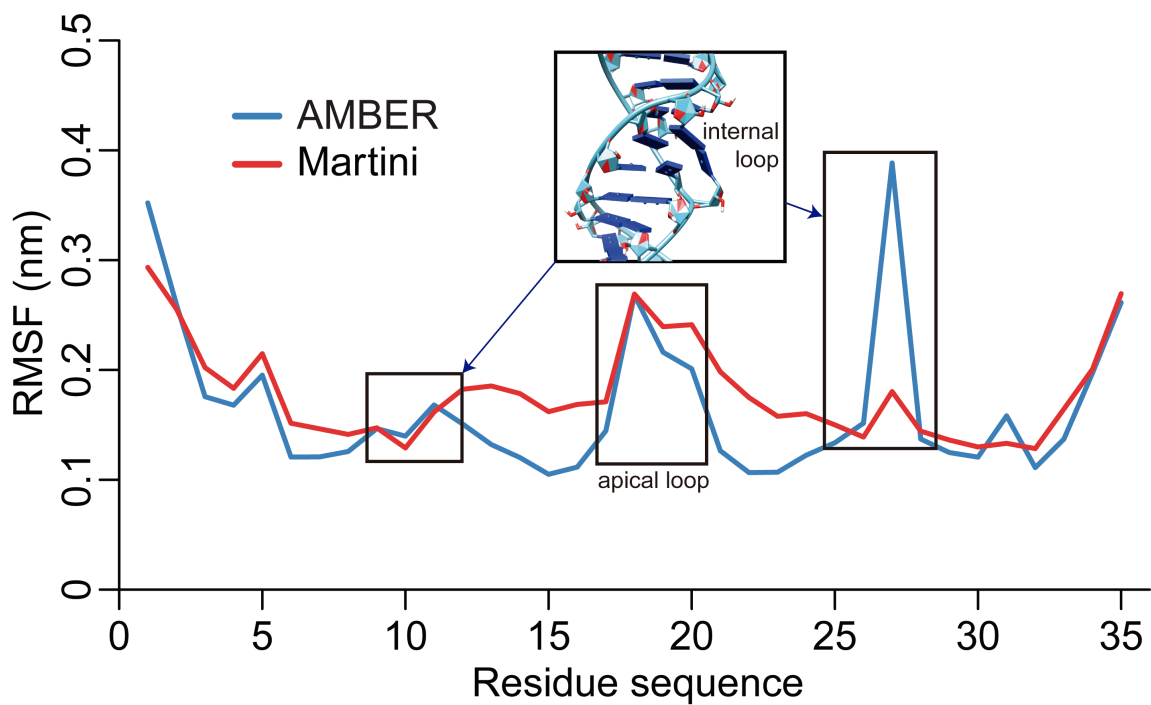


Figure S7. Local flexibility of the RNA containing a long internal and an apical loops

(PDB-ID 4FNJ). The root-mean-square fluctuations (RMSF) are visibly increased in the apical loop (residues 17-21) and in one of the long internal strands (9-12 and 26-28).

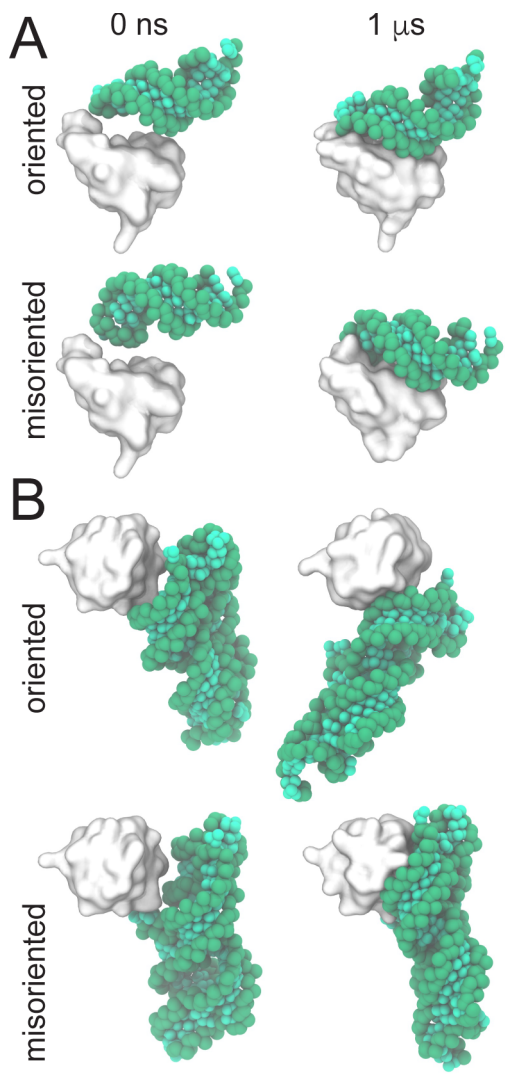


Figure S8. Spontaneous binding of RNA and protein with CG simulations. Initial and final snapshots after 1 μ s simulation time of the protein 19 of the human signal recognition particle (SRP19) in a complex with helix 6 of the Human SRP RNA (PDB-ID: 1JID) (A) and the SRP19 protein with the 7S.S RNA from the thermophilic methanogenic archaea (*M. jannaschii*) (PDB-ID: 1LNG) (B). Two relative orientations were used to simulate spontaneous binding: a 1 nm distant initial configuration between RNA and protein molecules ('oriented') and another with an additional 90° rotation ('misoriented'). A small fraction of the native contacts was recovered.